Fermi National Accelerator Laboratory

FN-393
0100.000
(Submitted to Physica D)

CATASTROPHE AND MAXWELL SURFACES OF THE HALF INTEGER RESONANCE EXCITED BY QUADRUPOLES AND OCTUPOLES

L. Michelotti

November 1983

Operated by Universities Research Association Inc. under contract with the United States Department of Energy

Catastrophe and Maxwell surfaces of the half integer resonance excited by quadrupoles and octupoles

Leo Michelotti

Fermi National Accelerator Laboratory

P.O. Box 500

Batavia, Illinois 60510

Abstract

The dynamics of a half integer resonance excited by quadrupoles and octupoles are classified by mapping the catastrophe and Maxwell surfaces of its Hamiltonian. Procedures for generating these surfaces are presented, and generic separatrices associated with some regions of the control space are displayed.

One standard way of extracting particles from an accelerator is to excite a half integer resonance with quadrupole and octupole magnets. By introducing a suitably scaled set of variables, the physics of this process can be idealized by a Hamiltonian of the following form.

$$H = [\nu+\cos(2\alpha+\phi)]J+[\kappa+\cos 2\alpha]J^2$$

$$= \frac{1}{4}(p^2+q^2)[p^2(\kappa+1)+q^2(\kappa-1)]$$

$$+ \frac{1}{2}(\nu+\cos\phi)p^2+\frac{1}{2}(\nu-\cos\phi)q^2-pq\sin\phi. \tag{1}$$

where $q = \sqrt{2J}\sin\alpha$, $p = \sqrt{2J}\cos\alpha$.

The three control variables, ν, κ, and ϕ are related to the distributions and strengths of the quadrupoles and octupoles around the accelerator: ν is the difference between the tune and the half integer n/2 scaled by the nth harmonic quadrupole driving term, κ is the ratio of 0th to nth harmonic octupole driving terms, and ϕ is the relative phase between the octupole and quadrupole harmonics. The dynamical variable q represents horizontal displacement from an equilibrium orbit, scaled by betatron functions and by the ratio of quadrupole to octupole harmonics; p is its conjugate momentum. The angle-action pair (α,J) are conjugate as well.

We will classify the dynamics of this system by mapping its transition boundary, the catastrophe and Maxwell surfaces. The Hamiltonian possesses three conspicuous symmetry transformations.

1. $\alpha\to\alpha+\pi$: All phase space flows are symmetric under inversion.
2. $\phi\to-\phi$; $\alpha\to-\alpha$: The flow at $2\pi-\phi$ is obtained from that at ϕ through a reflection across the p-axis.

3. $\alpha\to\alpha+\pi/2$; $\kappa\to-\kappa$; $\nu\to-\nu$; $h\to-h$: The flow at $(-\nu,-\kappa)$ is obtained from that at (ν,κ) by a 90° phase space rotation and time-reversal.

Because of the last two we need explore only half of the control space explicitly.

The topography of the transition boundary can be envisaged most easily by sectioning it at constant values of ϕ. Eight such sections are shown in Figure 1; the solid lines indicate the catastrophe surface, and the dashed lines, the Maxwell surface. The latter lies in the elliptically cross-sectioned tube

$$\nu^2-2\nu\kappa\cos\phi+\kappa^2 = \sin^2\phi.$$

The former is a more complicated surface consisting of two major pieces. The first is independent of ϕ and contains the planes $\nu = \pm1$ and $\kappa = \pm1$. These determine the flow characteristics at the origin and at infinity, as we shall see shortly. The second grows out of the corners $\nu = \kappa = \pm1$ as ϕ increases. It remains confined to the unit square when $\phi\varepsilon[0,\pi/2]$ but then leaks into the regions $|\omega|>1$, forming a cusp at its extremes. It begins to intersect itself at $\phi = 5\pi/6$, and eventually attaches itself to the two straight lines $2\kappa+\nu = \pm1$ when $\phi = \pi$.

Figure 2 and Figure 3 show how the dynamical possibilities are organized on the sections at $\phi = 0$ and $\phi = \pi$. The former encloses nine regions possessing five generically different classes of behavior; the latter, eighteen regions, with seven classes. The origin is stable or unstable accordingly as $|\nu|>1$ or $|\nu|<1$ (the latter inequality expresses the half-integer stop band in our units); separatrices are closed or open in phase space accordingly as $|\kappa|>1$ or $|\kappa|<1$. These transitions occur for all values of ϕ, but at $\phi = 0$, they are the only ones possible. On the Maxwell boundary at $\phi = \pi$ the separatrix consists of two straight lines intersecting at and a circle centered at the origin. No separatrix is associated with the regions ν, $\kappa > 1$ and ν, $\kappa < 1$ because there are no unstable fixed points there.

In the intervening region, the dynamical effects of crossing transition boundaries are appreciated best by following paths in the control space. Figure 4, for example, illustrates what happens along part of the path $(\nu, \kappa, \phi) = (-0.6, 0.4, 0..\pi)$. In going from $\phi = 0$ to $\phi = 150°$, the system does not cross a transition boundary, so separatrices at 4a are still diffeomorphic to two intersecting lines. Passage through the catastrophe surface at 4b and at 4d is signalled in phase space by the creation of a symmetric pair of degenerate, non-Morse fixed points, each appearing as a cusp in some trajectory. Those trajectories become new branches of the separatrix as each degeneracy splits into a stable-unstable pair of normal fixed points.

A "soft" transition occurs when the system crosses the Maxwell surface at 4f. The Hamiltonian at the unstable fixed points created at 4b takes on the value zero, and those branches merge with the one passing through the origin. They fall apart again at 4g, but a transition has occurred: the flows 4e and 4g are not generically equivalent. In particular, the latter contains trajectories which wind around the origin --- even though the origin is unstable ---- while the former does not. However, this transition has taken place without passing through a catastrophe. The fixed points are always Morse type fixed points, they are always the same in number and of the same character. This kind of transition has a non-local character. That is, it cannot be characterized by what happens at one point of phase space. A minimal characterization requires equating the value of the Hamiltonian at two separated, unstable fixed points.

As the system point approaches $\phi = \pi$, the stable areas created at 4d continue to expand until another merger takes place and we end up with the separatrix of Figure 3h.

Another example, this time along a path at constant ϕ, is presented in Figure 5. At the endpoints the flows are diffeomorphic to that of Figure 2a, because all three of these points can be connected without crossing the transition surface. Crossing the boundary at 5b creates degenerate fixed points and new separatrix branches that encircle stable fixed points, as shown. As the system moves from 5b to 5f each unstable fixed point separates itself from its stable partner and travels across to attach itself to the other one, which of course annihilates it.

There are 12 stable dynamical classes in all. One can sketch the generic separatrix associated with any control point of interest by following a path from a known control point and keeping track of all transition crossings. However, we shall turn away from continuing this catalog in order to describe the procedure for mapping the catastrophe surface.

Fixed points are found by applying Hamilton's equations to Eq. (1) and setting time derivatives to zero. This yields the following expressions.

$$J_0 = -\sin(2\alpha_0+\phi)/\sin(2\alpha_0)$$

$$\sin(2\alpha_0)[\nu+\cos(2\alpha_0+\phi)] = \sin(2\alpha_0+\phi)[\kappa+\cos(2\alpha_0)]. \quad (2)$$

The latter looks messy but is solved easily by writing it as a monic fourth order polynomial. We introduce the complex variables

$$z = e^{2i\alpha_0} \quad , \quad y = e^{-i\phi}$$

and rewrite Eq. (2) in a form that we shall call the "fixed point polynomial", or "fpp" for short.

$$\mathrm{fpp}(z) = \sum_{k=0}^{4} a_k z^k = 0, \tag{3a}$$

$$a_4 = 1 \ , \ a_2 = 3(1-y^2) \ , \ a_o = -y^2$$

$$a_3 = 4\kappa-2y\nu \quad , \quad a_1 = 2y\nu-4y^2\kappa. \tag{3b}$$

A catastrophe occurs when fixed points coalesce. Thus, on the catastrophe surface the fixed point polynomial must have a unimodular solution of multiplicity two, or greater. Accordingly, it can be factorized

$$\mathrm{fpp}(z) = (z-u)^2 (z-v) (z-w) \tag{3c}$$

where $|u| = 1$, in order that α_o be real. The fpp coefficients, written in terms of these solutions, are

$$\begin{aligned} a_3 &= -(v+w+2u) \\ a_2 &= u^2+vw+2u(v+w) \\ a_1 &= -u^2(v+w) - 2uvw \\ a_0 &= u^2vw. \end{aligned} \tag{4}$$

To map this as a surface in control space we must invert Eq's. (3b), according to

$$y^2 = -a_0$$

$$\kappa = \frac{3}{4}\;\frac{a_1+a_3}{a_2} \tag{5}$$

$$y\nu = 2\kappa - a_3/2. \tag{6}$$

It will be possible to do this and to interpret the answers as real, physical quantities only if the coefficients satisfy three "realizability conditions" which follow immediately from Eq's. (3b).

1. $|a_0| = 1$, (ϕ must be real) (7a)

2. $\frac{1}{3}\, a_2 - a_0 = 1$ (7b)

3. $a_1 = a_0 a_3^{*}$. (7c)

We shall show below that the first two conditions are sufficient as well as necessary by proving that they imply the third and that the control variables obtained are real. This statement is made formal in the following.

<u>KEY PROPOSITION</u> If a monic fourth order polynomial has a degenerate unimodular solution and satisfies the first two realizability conditions, then (a) it satisfies the third realizability condition, and (b) it is the fpp of a real valued control point, (ν,κ,ϕ).

Sections of the catastrophe surface are calculated in the following manner. Eq. (7b), in conjunction with Eqs. (4) implies that

$$u^2(\tfrac{1}{3} - vw) + \tfrac{2}{3}u(v+w) + (\tfrac{1}{3}vw - 1) = 0. \tag{8}$$

Now, ϕ = constant is equivalent to $a_o = -y^2 = u^2vw$ = constant. Use this to eliminate w in Eq. (8); the resulting polynomial is quadratic in v.

$$(uy^*)v^2 + \tfrac{1}{2}[u^2y^* - u^{*2}y - 3(y^* - y)]v - u^*y = 0. \tag{9}$$

An "algorithm" can now be sketched, in pidgin algol, as follows:

```
for "all" φε(0,π)
begin: y : = exp(-iφ);
       for "all" u on unit circle
       begin: solve Eq. (9) for v+ and v-;
              for v = {v+,v-}
              begin: w : = -y²/u²v;
                     J₀ : = (y²-u²)/y(u²-1)
                     if J₀>0 then evaluate and plot
                                  (ν,κ) using Eq. (5) and Eq. (6);
              end;
       end;
end;
```

The test $J_o>0$ must be done explicitly; only if this inequality is satisfied does the control point produce a real non-Morse fixed point.

The algorithm does not handle the endpoints $\phi = 0$ and $\phi = \pi$, because κ evaluates to 0/0. For $\phi = 0$, J_0 is always negative so nothing more need be done. At $\phi = \pi$ we have $y = -1$, $a_0 = 1$, $a_2 = 0$, and $a_3 = -a_1 = 4\kappa+2\nu$. The fpp factorizes immediately.

$$fpp(z) = (z-1)(z+1)(z^2+a_3z+1).$$

Now, a_3 must be chosen so that there is at least one degenerate solution. The possibilities are

(a) z^2+a_3z+1 is a perfect square. This means that either

(a.1) $a_3 = +2$, and $fpp(z) = (z-1)(z+1)^3$, or

(a.2) $a_3 = -2$, and $fpp(z) = (z-1)^3(z+1)$.

(b) $(z+1)|(z^2+a_3z+1)$

This reduces to case (a.1).

(c) $(z-1)|(z^2+a_3z+1)$

This reduces to case (a.2).

In all cases we have $a_3 = \pm 2$, or equivalently, $2\kappa+\nu = \pm 1$. Further, the non-Morse solution is triply degenerate; that is, it corresponds to the merger of three fixed points.

Finally we prove the "key proposition". Begin with the following lemma, which assumes the hypothesis of the key proposition.

LEMMA: $vw = (v+w)/(v+w)^*$ (v,w as defined in Eq. (3c))

PROOF: Because of the first realizability condition, and $|u| = 1$,

$$|vw| = |u|^2|vw| = |u^2vw| = |a_0| = 1. \tag{10}$$

Now, multiply Eq. (8) by $3u^*$ to get

$$u(1-3vw)+2(v+w)+u^*(vw-3) = 0.$$

Take the complex conjugate, multiply by vw, and use Eq. (10) to get

$$u(1-3vw)+2vw(v+w)^{*}+u^{*}(vw-3) = 0.$$

Subtracting these two expressions yields the desired result. ■

<u>PROOF OF THE KEY PROPOSITION</u>

part (a)

Using Eq's. (4) and the lemma we calculate

$$\begin{aligned} a_1 &= -u^2(v+w)-2uvw \\ &= -u^2vw[(vw)^{*}(v+w)+2u^{*}] \\ &= y^2[(v+w)^{*}+2u^{*}] \\ &= a_0a_3^{*} \end{aligned}$$

part (b)

First, κ is real iff$(a_1+a_3)(1+a_0^{*})$ is real, according to Eq. (5). But, using what we've proved in part (a).

$$\begin{aligned} (a_1+a_3)(1+a_0^{*}) &= (a_3-y^2a_3^{*})(1-y^{*2}) \\ &= (y^{*}a_3-ya_3^{*})(y-y^{*}) \end{aligned}$$

which is manifestly a real quantity. On the other hand, using Eq. (6)

$$\begin{aligned} 2\nu|1-y^2|^2 &= (a_3+a_1y^{*2})(y-y^{*}) \\ &= (a_3-a_3^{*})(y-y^{*}) \end{aligned}$$

which again is manifestly real. ■

ACKNOWLEDGEMENT

It is a pleasure to acknowledge the discussions I have had with Dr. D. Edwards of Fermilab, who introduced me to the subject of half integer extraction.

REFERENCES

1) R. Gilmore, Catastrophe Theory for Scientists and Engineers, John Wiley and Sons, New York, 1981.

2) L.P. Michelotti and S. Ohnuma, "Dipole Shuffling in the Fermilab Energy Saver", IEEE Trans. on Nuc. Sci. NS-30 (4), 2472 (Aug., 1983).

3) G. Guignard, "A General Treatment of Resonances in Accelerators", CERN 78-11, European Organization for Nuclear Research, Geneva, Switzerland (10 Nov 1978).

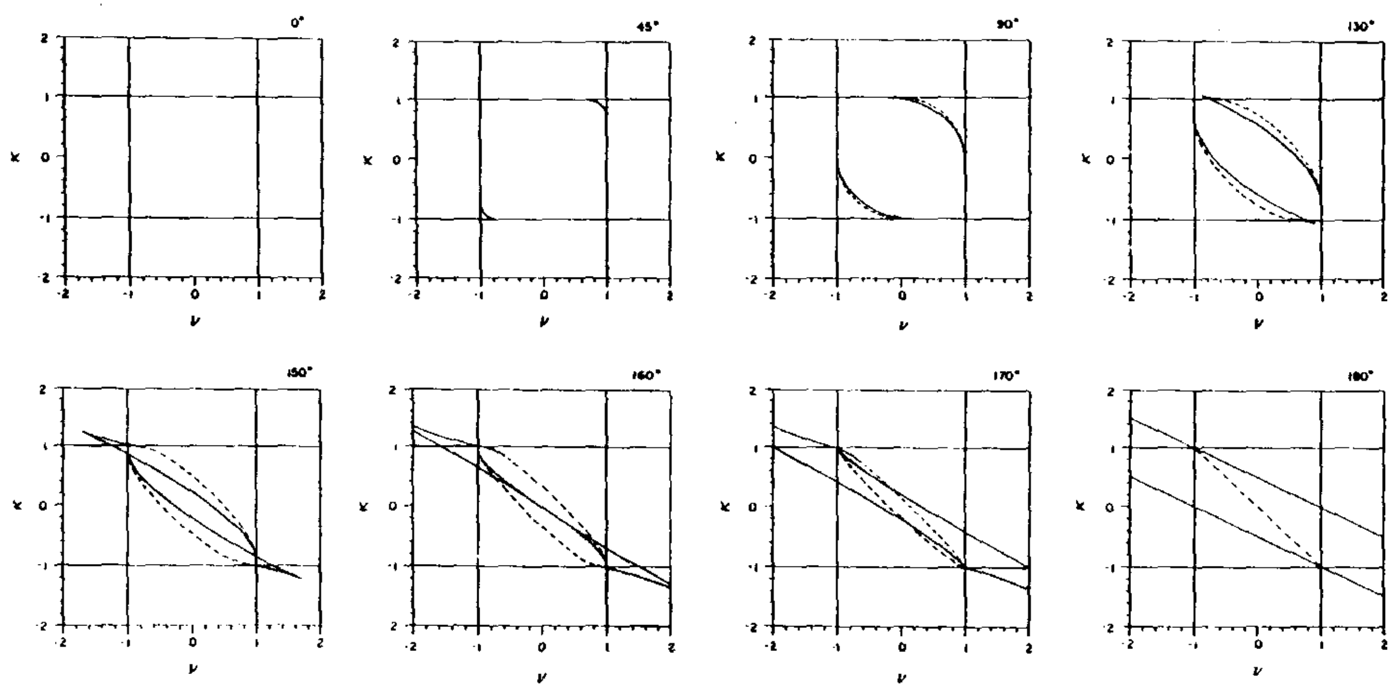

Figure 1 Sections of the catastrophe and Maxwell surfaces at constant values of ϕ.

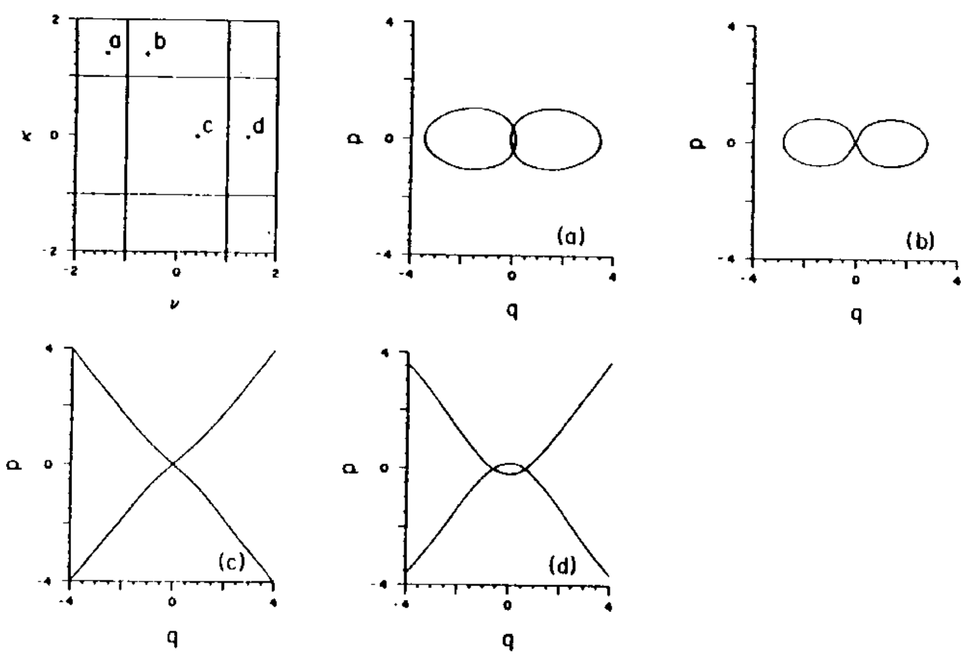

Figure 2 Generic separatrices at the control plane $\phi = 0$.

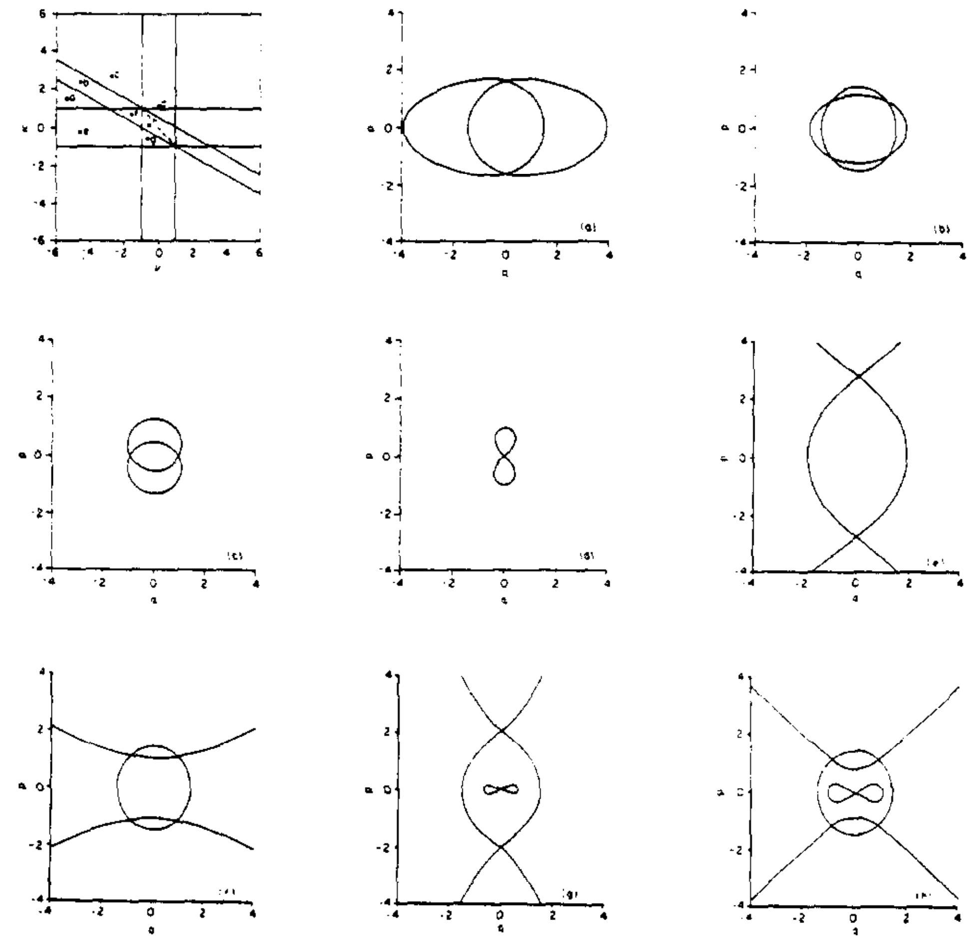

Figure 3 Generic separatrices at the control plane ϕ = 180°.

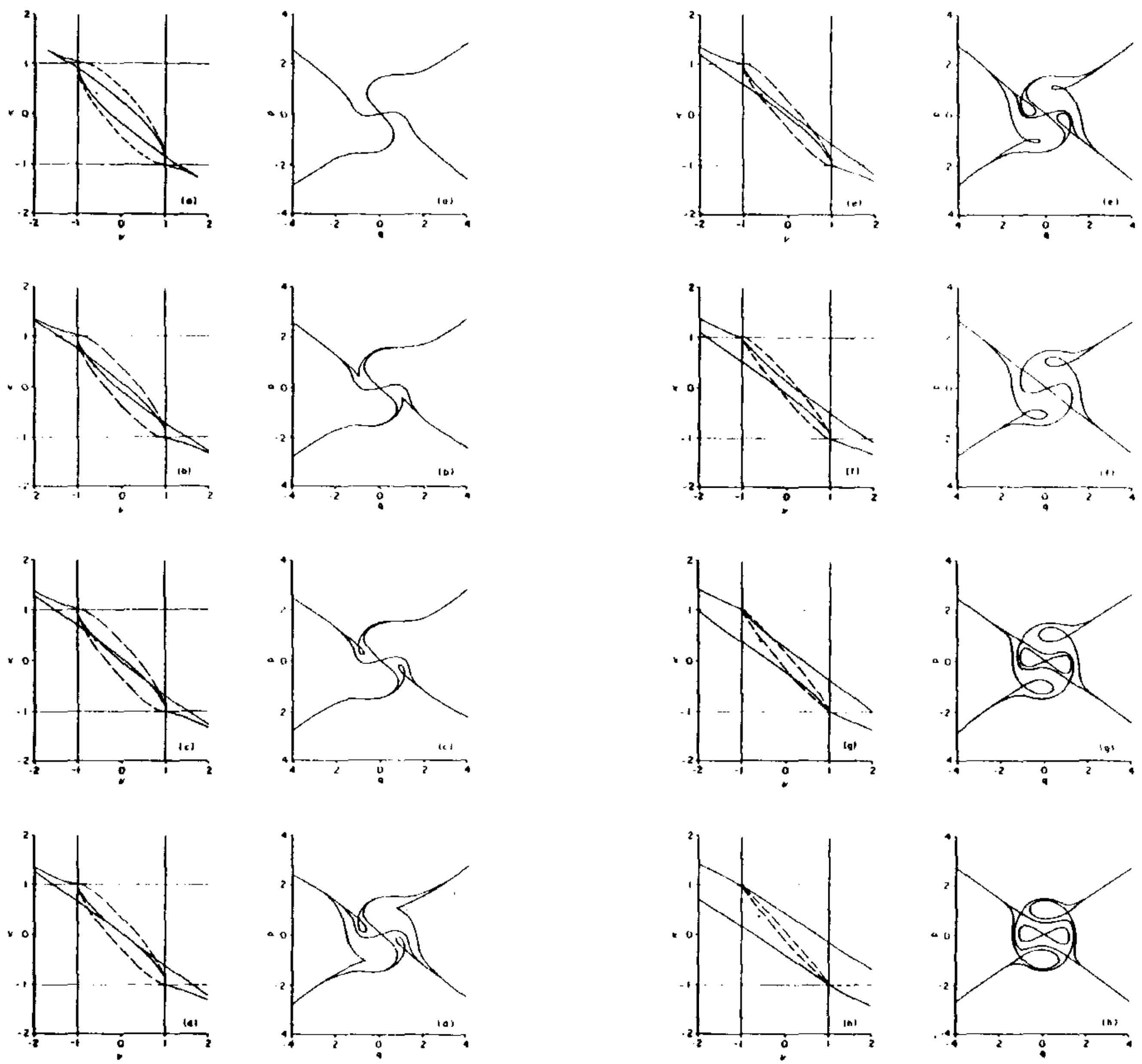

Figure 4   Following the dynamics along a control path at constant $(\nu,\kappa) = (-0.6,0.4)$.

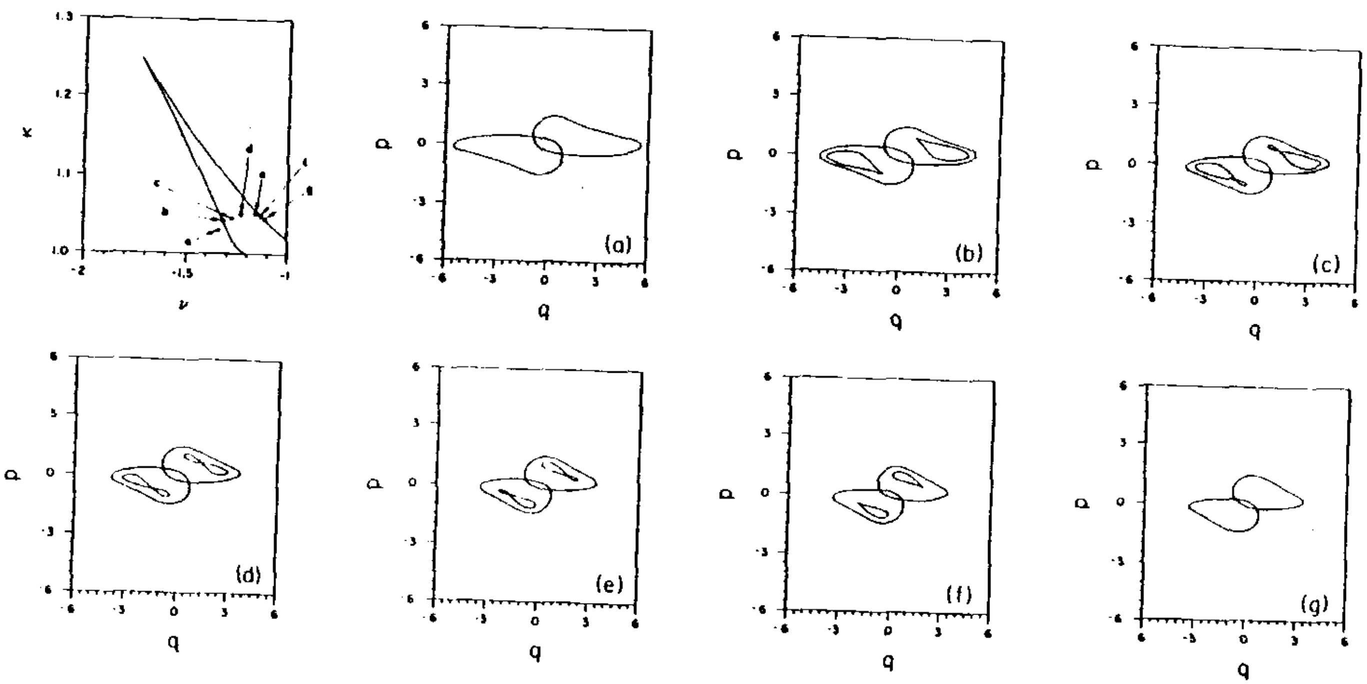

Figure 5 Following the dynamics along a control path at constant $\phi = 150°$. (Note the enlarged scale of the control space diagram,)